

Gravitational Imprints of Flavor Hierarchies

Admir Greljo,^{1, a} Toby Opferkuch,^{1, b} and Ben A. Stefanek^{2, c}

¹*Theoretical Physics Department, CERN, 1211 Geneva, Switzerland*

²*PRISMA Cluster of Excellence and Mainz Institute for Theoretical Physics,
Johannes Gutenberg-Universität Mainz, 55099 Mainz, Germany*

(Dated: October 7, 2019)

The mass hierarchy among the three generations of quarks and charged leptons is one of the greatest mysteries in particle physics. In various flavor models, the origin of this phenomenon is attributed to a series of hierarchical spontaneous symmetry breakings, most of which are beyond the reach of particle colliders. We point out that the observation of a multi-peaked stochastic gravitational wave signal from a series of cosmological phase transitions could well be a unique probe of the mechanism behind flavor hierarchies. To illustrate this point, we show how near future ground- and space-based gravitational wave observatories could detect up to three peaks in the recently proposed PS^3 model.

I. INTRODUCTION

The first direct detection of gravitational waves (GW) [1] was a stunning confirmation of the theory of general relativity and marked the discovery of the only messenger via which the universe can be probed back to the Planck era. To take advantage of this unique window into the universe, the next few decades will see a plethora of ground- and space-based gravitational wave observatories being built across twelve decades in frequency [2–9]. In addition to what can be learned on the astrophysical front, this experimental effort offers an immense opportunity to probe fundamental physics in the early universe. Indeed, many particle physics processes that produce a stochastic gravitational wave background have already been identified, such as the primordial spectrum expected from inflation [10–12], violent first order phase transitions (FOPTs) [13–35], cosmic strings [36–39], non-perturbative particle production [40–46], primordial black holes [47–49], etc. Many of these processes are expected to produce a GW spectrum with a single peak, with the notable exception being the nearly scale-invariant spectrum from inflation.

Not as frequently discussed is the possibility of observing a multi-peaked gravitational wave signal, in either single or multiple experiments, and what such a signal might tell us about open puzzles in fundamental physics. One intriguing possibility is that a multi-peaked signal could come from a series of sequential FOPTs. As the peak frequency of the GW spectrum from a first order phase transition is set by the vacuum expectation value (VEV) in the broken phase, the observation of a multi-peaked signal could contain information about the scales of multiple spontaneous symmetry breakings (SSBs), with the first breaking giving the highest frequency peak and the last the lowest.

A longstanding question within fundamental physics is that of the flavor puzzle, which refers to why the Standard Model (SM) fermion Yukawa couplings are spread over so many orders of magnitude, with a top quark Yukawa that is $\mathcal{O}(1)$ but an electron Yukawa which is five orders of magnitude smaller. Just the quark sector alone has a hierarchy which covers 4-5 decades and also contains the puzzle of why the CKM mixing matrix is close to identity.

It has been proposed that the flavor hierarchies could be generated via a series of hierarchical SSBs [50–60]. These types of models typically associate flavor with a fundamental gauge symmetry at high energies. The SM fermion masses and mixings are then generated via spontaneous breaking of this gauge symmetry, usually in several steps. The aforementioned models are compatible with the lowest SSB occurring at the TeV scale, which is highly motivated as it is the scale currently being probed at colliders (perhaps also in order to explain flavor anomalies [61–69]). Interestingly enough, if this breaking occurs via a strongly FOPT, the resulting GW signal is in the sensitivity range of upcoming space-based interferometers such as LISA. Moreover, the higher breakings associated with light family mass generation may produce GW in the range of future ground-based interferometers such as Einstein Telescope (ET) and Cosmic Explorer (CE). Such a scenario would lead to a spectacular signature involving a multi-peaked GW signal, the peak frequencies of which contain information about the flavor hierarchies, spread across future GW experiments covering four decades of frequency space. This separation in frequency can be roughly seen by taking the geometric mean of the quark masses of each family,

$$\begin{array}{lll} \sqrt{m_t m_b} & : & \sqrt{m_s m_c} & : & \sqrt{m_u m_d} \\ 1 & : & 10^{-2} & : & 10^{-4} \\ f_{\text{LISA}}^{-1} & : & \dots & : & f_{\text{ET}}^{-1} \end{array}$$

To further develop this idea, we will take the PS^3 model of Ref. [60] as a concrete example in what follows, though the concept generalizes to many models which solve the flavor puzzle through a series of hierarchical SSBs.

^a admir.greljo@cern.ch

^b toby.opferkuch@cern.ch

^c bstefan@uni-mainz.de

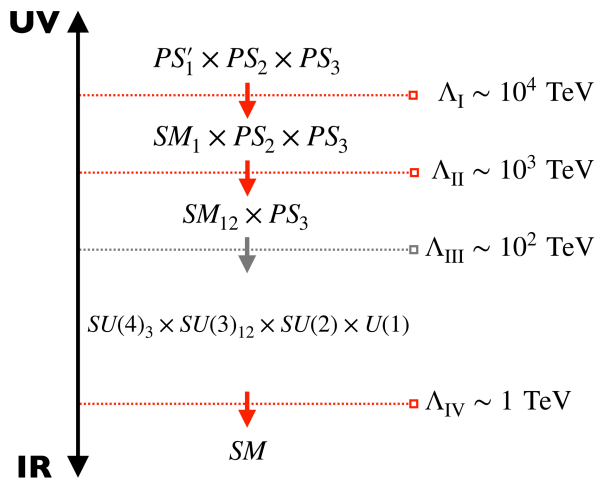


FIG. 1. Schematic view of the PS^3 model detailed in Section II. Phase transitions marked with red arrows correspond to $SU(4)$ breakings (see Section III).

II. MODEL EXAMPLE: PATI-SALAM CUBED

As a prototypical example, we focus on the PS^3 model first introduced in Ref. [60].¹ Here, the original Pati-Salam gauge group [75] in higher-dimensional spacetime is deconstructed [76] onto three four-dimensional sites $PS^3 \equiv PS_1 \times PS_2 \times PS_3$, where each copy acts on one family of SM fermions. In particular, an entire SM family including the right-handed neutrino fits into two left- and right-chiral multiplets, $\Psi_L^{(i)} \equiv (\mathbf{4}, \mathbf{2}, \mathbf{1})_i$ and $\Psi_R^{(i)} \equiv (\mathbf{4}, \mathbf{1}, \mathbf{2})_i$, which embed quark and lepton doublets $Q_L^{(i)}$ and $L_L^{(i)}$ and singlets $u_R^{(i)}$, $\nu_R^{(i)}$, $d_R^{(i)}$ and $e_R^{(i)}$, respectively. The label $i = 1, 2, 3$ denotes the corresponding gauge group $PS_i \equiv [SU(4) \times SU(2)_L \times SU(2)_R]_i$.

The model undergoes a series of SSBs occurring at different energy scales as illustrated in Fig. 1. The first breaking after inflation is triggered by the VEV of Σ_1 in $\mathbf{4}$ of $SU(4)_1$.² The subsequent breakings to the diagonal subgroups of neighboring sites are achieved by the appropriate scalar link fields in bifundamental representations, $\Phi_{ij}^{L,R}$ and Ω_{ij} . More specifically, Φ_{ij} 's are in $\mathbf{2}$ of the corresponding $SU(2)_i$ and $\mathbf{2}$ of $SU(2)_j$, while similarly, Ω_{ij} is $(\mathbf{4}, \mathbf{2}, \mathbf{1})_i \times (\mathbf{4}, \mathbf{2}, \mathbf{1})_j$. Finally, the Higgs fields live at the third site, e.g. $H_3 \equiv (\mathbf{1}, \mathbf{2}, \mathbf{2})_3$.

Below the scale Λ_{II} , the unbroken phase of the theory, $SM_{12} \times PS_3$, leads to an approximate $U(2)$ flavor symmetry observed in the SM at low-energies [78].

The lower bound on this scale, $\Lambda_{II} \gtrsim 10^3$ TeV, follows from stringent limits on flavor changing neutral currents (FCNC) induced by the heavy gauge bosons coupling to the first two generations [79–83]. At this level, Yukawa interactions are only allowed for the third family, $\mathcal{L} \supset \bar{\Psi}_L^{(3)} H_3 \Psi_R^{(3)}$, predicting vanishing light-fermion masses and a CKM matrix equal to identity. The smallness of neutrino masses is achieved by the inverse seesaw mechanism [71]. The perturbation to this picture is obtained by higher-dimensional operators such as

$$\begin{aligned} \mathcal{L}_{23} &= \frac{1}{\Lambda_{III}} \bar{\Psi}_L^{(2)} \Omega_{23} H_3 \Psi_R^{(3)} + \text{h.c.}, \\ \mathcal{L}_{12} &= \frac{1}{\Lambda_{II}^2} \bar{\Psi}_L^{(k)} \Phi_{k3}^L H_3 \Phi_{3l}^R \Psi_R^{(l)} + \text{h.c.}, \end{aligned} \quad (1)$$

after the link fields acquire VEVs. The leading $U(2)$ breaking spurion, following from the first term, generates the mixing of the third and light families, $|V_{ts}| \sim \langle \Omega_{23} \rangle / \Lambda_{III}$, where $\langle \Omega_{23} \rangle \sim \Lambda_{IV}$. The light fermion masses are instead due to the second term, with the largest being $y_c \sim \langle \Phi_{23}^L \rangle \langle \Phi_{32}^R \rangle / \Lambda_{II}^2$. Similarly, y_u follows from Λ_I , etc. The UV completion of the effective operators in Eq. (1) has been discussed in Refs. [60, 71]. We assume the scales generating the operators to coincide with the preceding symmetry breaking scales, e.g. $\Lambda_{III} \sim \langle \Phi_{23} \rangle$ and $\Lambda_{II} \sim \langle \Phi_{12} \rangle$. From here it follows that the four-step breaking, *i*) 10^4 TeV, *ii*) 10^3 TeV, *iii*) 10^2 TeV, and *iv*) 1 TeV, is well compatible with the observed pattern of fermion masses and mixings at low-energies.³ As we will show later, the three $SU(4)$ phase transitions naturally induce a stochastic GW signature within the reach of next-generation interferometers.⁴

While we work in the deconstructed four-dimensional picture, the higher-dimensional model relates the hierarchy of quark and charged lepton masses to the stabilization mechanism of branes in the bulk [84]. Additionally, the higher-dimensional gauge symmetry justifies small scalar quartic couplings [85] leading to an almost classically scale invariant potential which is crucial to ensure strongly FOPTs as shown later.

III. GRAVITATIONAL WAVE CALCULATION

A. Effective Potential

To describe the first SSB in PS^3 at the scale Λ_I , we calculate in a simplified $4 \rightarrow 3$ model where $SU(4)$ is

¹ This is arguably the most compelling UV picture which offers a coherent explanation of the current flavor anomalies. See e.g. [70–74].

² We propose a slight variation of the original model breaking $[SU(2)_R]_1$ before inflation effectively solving the monopole problem of low-scale PS models [77]. PS'_1 in Fig. 1 is defined as $[SU(4) \times SU(2)_L \times U(1)]_1$.

³ Another independent argument to keep the first two SSBs close to the bounds implied by FCNC is to avoid large tuning of the Higgs mass which is only partially screened from the first two sites.

⁴ The $SU(2)$ breakings at the scale Λ_{III} may also produce stochastic GW signatures, but lie in a suboptimal frequency range for LISA and ET. This provides additional motivation for proposed intermediate frequency experiments such as atom interferometers or DECIGO.

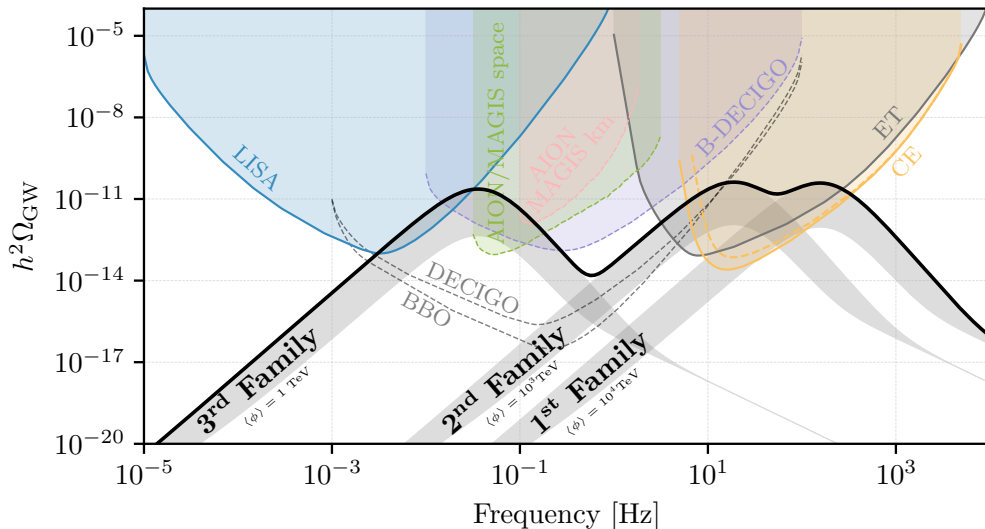


FIG. 2. Complete GW spectrum, which we term the *Triglav signature*, following from three FOPTs in the PS^3 model. See Section III C for details.

broken to $SU(3)$ by the VEV of a complex scalar Σ in the fundamental representation of $SU(4)$. The matter content includes one set of doublets Ψ_L and Ψ_R , also in the fundamental representation of $SU(4)$. In the PS^3 model, scalar fields which break $SU(4)$'s have suppressed Yukawa interactions and scalar cross-quartics⁵. As a result, the relevant part of Lagrangian for the GW calculation depends only on a few parameters. More explicitly,

$$\mathcal{L} = \bar{\Psi} i \not{D} \Psi - \frac{1}{4} (F_{\mu\nu}^a)^2 + |D_\mu \Sigma|^2 + \lambda v^2 |\Sigma|^2 - \lambda |\Sigma|^4, \quad (2)$$

with $D_\mu = \partial_\mu - ig A_\mu^a T^a$. Thus, the relevant parameters of the model are g , λ , and v . The breaking $SU(4) \rightarrow SU(3)$ occurs when the complex scalar Σ acquires a VEV of the form $\langle \Sigma \rangle = (0, 0, 0, v/\sqrt{2})^T$. The 7 broken generators correspond to a massive vector leptoquark U_μ and Z' gauge boson. The decomposition of Σ under the unbroken $SU(3)$ is $\mathbf{4} = \mathbf{3} + \mathbf{1}$, with the entire complex $\mathbf{3}$ and the imaginary part of $\mathbf{1}$ containing the leptoquark and Z' goldstones, respectively. The remaining degree of freedom $\text{Re } \Sigma_4 \equiv \phi/\sqrt{2}$ is a massive radial mode. The full finite-temperature effective potential for ϕ is

$$V_{\text{eff}}(g, \lambda, v, \phi, T) = V_0 + V_{CW} + V_{T \neq 0}, \quad (3)$$

where tree level potential V_0 is

$$V_0(\lambda, v, \phi) = -\frac{1}{2} \lambda v^2 \phi^2 + \frac{\lambda}{4} \phi^4. \quad (4)$$

⁵ The higher-dimensional operators generating Yukawa interactions in Eq. (1) give a negligible correction to the effective potential.

The one-loop Coleman-Weinberg correction V_{CW} is

$$V_{CW}(g, \lambda, v, \phi) = \sum_b n_b \frac{m_b^4(\phi)}{64\pi^2} \left(\ln \frac{m_b^2(\phi)}{\mu_R^2} - C_a \right), \quad (5)$$

which we have written here in Landau gauge using the $\overline{\text{MS}}$ renormalization scheme which gives $C_a = 3/2$ ($5/6$) for scalars (gauge bosons). The sum on b is over all bosons which have a ϕ -dependent mass and n_b is the total number of degrees of freedom of the boson. The final piece $V_{T \neq 0}$ is the finite temperature correction to the potential

$$V_{T \neq 0}(g, \lambda, v, \phi, T) = \frac{T^4}{2\pi^2} \sum_b n_b J_b \left(\frac{m_b^2(\phi) + \Pi_b(T)}{T^2} \right), \quad (6)$$

which includes a correction from resummed Daisy diagrams. The thermal function $J_b(x^2)$, the ϕ -dependent masses $m_b(\phi)$, and the Debye masses $\Pi_b(T)$ are all given in the supplemental material. As we will show later, in the PS^3 model with $g \sim \mathcal{O}(1)$ and small λ , $V_{T \neq 0}$ naturally induces a thermal barrier which leads to a strong FOPT.

The subsequent $SU(4)$ transitions at the scales Λ_{II} and Λ_{IV} are modeled by the more complicated breaking pattern $SU(4) \times SU(3)' \rightarrow SU(3)$ which is presented in the supplemental material.

B. Numerical Procedure

The GW spectrum from a FOPT is described by four parameters [2, 86–88]. These are the nucleation temperature T_n which describes the onset of the phase transition, the strength α , the inverse timescale β , and the

bubble wall velocity v_w . Due to gauge bosons in the plasma with sizeable couplings to the bubble walls and a strongly FOPT, we are in the regime of non-runaway bubbles with $v_w \sim 1$ where the peak of the GW spectrum is determined by the sound wave contribution [2]. The remaining parameters we compute from the effective potential in Eq. (3) using the `CosmoTransitions` [89] package, the results of which we have confirmed using our own code based on the method of Ref. [90]. Thus, for a given set of model parameters g, λ, v we compute the corresponding GW parameters α, β, T_n which allows us to obtain the GW spectrum from a template function extracted from lattice simulation [91–93]. We then are able to perform a standard signal-to-noise ratio (SNR) analysis to determine the detectability of the signal, see e.g. Ref. [94]. More details can be found in the supplemental material.

C. Results

We show in Fig. 2 a benchmark multi-peaked GW signal where the first two transitions would be detectable in ET/CE and the final TeV scale phase transition would be detectable in LISA. Remarkably, the predicted PS^3 symmetry breaking scales (Fig. 1) correspond to peak frequencies in the optimal range for experiments. The solid black line is the total signal which is the combination of the individual spectra and corresponds to the nominal LISA recommendation for modeling GW formation and propagation [2]. The gray bands correspond to a conservative treatment of the sound wave contribution which illustrates the amount of theoretical uncertainty.

In the benchmark signal of Fig. 2, different peaks are obtained by appropriately varying the VEVs ($1, 10^3, 10^4$ TeV), as well as the effective relativistic degrees of freedom in the plasma. The renormalization group evolution of PS^3 unambiguously determines the values of all gauge couplings at the relevant scales starting from the benchmark input $g_{4,3}(\Lambda_{IV}) = 2, g_{4,2}(\Lambda_{II}) = \sqrt{2}$, and matching to the strong coupling at the scale Λ_{IV} .⁶ The $SU(4)$ coupling at the third site $g_{4,3}(\Lambda_{IV})$ is chosen to be somewhat larger as suggested by the current flavor anomalies [72]. Finally, the three quartic couplings are set to $\lambda(\Lambda_{IV}) = 10^{-2}, \lambda(\Lambda_{II}) = 10^{-2}$, and $\lambda(\Lambda_I) = 0.5 \times 10^{-2}$.

To assess how generic GW signatures are in PS^3 , we show as an example in Fig. 3 the detectability of the GW spectrum computed in ET and CE, as a function of g and λ for a fixed VEV of 10^3 TeV. These regions were computed using our simplified $4 \rightarrow 3$ model to calculate the GW parameters and spectrum, after which a detectability analysis is performed where we require an

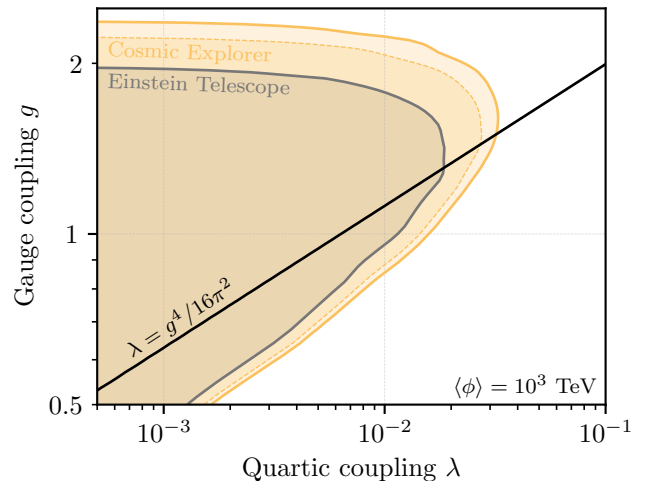


FIG. 3. Detectability of GW from a FOPT in the $4 \rightarrow 3$ simplified model. See Section III C for details.

SNR of 5 to obtain the boundaries. One can see immediately from Fig. 3 that significant parameter space exists which allows for a FOPT producing an observable GW signal without tuning. Furthermore, the best GW signatures are given for *i*) gauge couplings of $\mathcal{O}(1)$ and *ii*) small quartic coupling.

Interestingly enough as discussed in Section II, both of these conditions are generic predictions of PS^3 because *i*) it embeds the strong gauge group and *ii*) the natural size of the quartic is set by the one-loop Coleman-Weinberg correction from the gauge sector. Indeed, the solid black line of Fig. 3 which falls nicely into the detectable region shows the expected size of $\lambda \approx g^4/16\pi^2$ as would be generated from renormalization group flow. We have verified that $SU(4) \times SU(3)' \rightarrow SU(3)$ breaking pattern leads to qualitatively similar results.

IV. CONCLUSIONS

The peculiar pattern of hierarchical fermion masses which span many orders of magnitude is one of the longest standing puzzles in fundamental physics, the solution of which might require radical new approaches beyond colliders. In this letter we propose for the first time that a multi-peaked stochastic gravitational wave signature (where the ratios of peak frequencies follow the flavor hierarchies) could provide such a probe.

This idea is best illustrated in the context of the recently proposed PS^3 model for flavor hierarchies [60], motivated also in part by the current B -meson anomalies. Here, the successful quark-lepton unification of the original Pati-Salam model is made compatible with flavor data by dimensional deconstruction onto three sites, one for each generation of SM fermions.

We show that the parameters of the PS^3 model gener-

⁶ The breaking of $SU(4)_i \times SU(3)_j \rightarrow SU(3)$ implies the matching condition $g_3^{-2} = g_{4,i}^{-2} + g_{3,j}^{-2}$.

ically yield strongly first-order phase transitions as the gauge symmetry is sequentially broken down to the SM in hierarchical steps. Remarkably, the peak frequencies of the resulting GW spectra as determined by the VEVs fall precisely into the projected sensitivity range of future experiments. As we have argued, these are nearly inevitable predictions of the model as constructed. Such a spectacular signal, if observed, would offer a unique opportunity to probe the origins of the flavor hierarchies at energy scales which are currently inaccessible to colliders.

ACKNOWLEDGMENTS

We thank Kfir Blum, Moritz Breitbach, Javier Fuentes-Martín, Gino Isidori, Andrey Katz, Joachim Kopp, Pedro Schwaller, and Marko Simonović for insightful discussions. TO has received funding from the European Research Council (ERC) under the European Union’s Horizon 2020 research and innovation programme (grant agreement No. 637506, “ ν Directions”) awarded to Joachim Kopp.

Appendix A: Model Details

1. $SU(4) \rightarrow SU(3)$

The last remaining pieces to complete the $4 \rightarrow 3$ model of Section III A describing the Λ_I transition is the determination of both the field dependent masses and Debye masses. The relevant fields entering the sum in Eq. (3) are $b = \phi, S_0, S, Z'_\mu{}^T, U_\mu{}^T, Z'_\mu{}^L, U_\mu{}^L$ with the corresponding number of degrees of freedom $n_b = 1, 1, 6, 2, 12, 1, 6$, while their field-dependent masses are:

$$m_\phi^2 = 3\lambda\phi^2 - \lambda v^2, \quad m_{S_0, S}^2 = \lambda\phi^2 - \lambda v^2, \quad (\text{A1})$$

$$m_{Z'}^2 = \frac{3g^2\phi^2}{8}, \quad m_U^2 = \frac{g^2\phi^2}{4}. \quad (\text{A2})$$

The Debye masses in the high-temperature limit are obtain following Refs. [15, 95, 96], yielding

$$\begin{aligned} \Pi_\Sigma(T) &= \frac{5}{6}\lambda T^2 + \frac{15}{32}g^2 T^2, \\ \Pi_{A_\mu}^L(T) &= \frac{11}{6}g^2 T^2, \quad \Pi_{A_\mu}^T(T) = 0, \end{aligned} \quad (\text{A3})$$

where L and T label the longitudinal and transverse components of the gauge field.

2. $SU(4) \times SU(3) \rightarrow SU(3)$

The SSBs at the scales Λ_{II} and Λ_{IV} are described by an $SU(4) \times SU(3)$ gauge group broken by the complex scalar field $\Omega_3 = (\mathbf{4}, \mathbf{3})$ to the diagonal $SU(3)$ subgroup.

The decomposition of Ω_3 under the unbroken $SU(3)$ is

$$\begin{aligned} \Omega_3^{ij} &= \frac{1}{\sqrt{3}}S_3\delta_{ij} + \frac{1}{\sqrt{2}}O_3^a\lambda_{ij}^a, \\ \Omega_3^{4j} &= T_3^j. \end{aligned} \quad (\text{A4})$$

where $i, j = 1, 2, 3$, and λ_{ij}^a are the Gell-Mann matrices. S_3, T_3^j and O_3^a are a complex scalar singlet, triplet and octet, respectively. The real part of S_3 is the Higgs, while its imaginary part is the Z' goldstone. The VEV of $\mathbf{Re} S_3 = \phi/\sqrt{2} \equiv \sqrt{3}v_3/\sqrt{2}$ breaks the symmetry. T_3 is the goldstone of the vector leptokuark, while $\mathbf{Im} O_3$ is the goldstone of the coloron. Finally, $\mathbf{Re} O_3$ describes a physical scalar octet particle. In addition we require the following Dirac fermions: two copies of $(\mathbf{4}, \mathbf{1})$ and two copies of $(\mathbf{1}, \mathbf{3})$ which embed the SM fermions. However, these fermions do not have Yukawa interactions with Ω_3 and hence only contribute to the Debye mass for the gauge bosons.

In what follows, we neglect contributions from the small quartic couplings everywhere except in the tree-level potential. As a result we need only include the field-dependent and Debye masses for the vector bosons.⁷

For the transverse polarizations of the gauge bosons the relevant field dependent masses are:

$$m_{g'}^2 = \frac{(g_3^2 + g_4^2)\phi^2}{6}, \quad (\text{A5})$$

$$m_{U_1}^2 = \frac{g_4^2\phi^2}{12}, \quad m_{Z'}^2 = \frac{g_4^2\phi^2}{24}, \quad (\text{A6})$$

with corresponding degrees of freedom $n_b = 16, 12, 2$, respectively. For the longitudinal polarizations the Debye masses also play a role. These masses are:

$$\begin{aligned} SU(4) : \quad \Pi_{H_\mu}^L(T) &= \frac{13}{6}g_4^2 T^2, \\ SU(3) : \quad \Pi_{C_\mu}^L(T) &= 2g_3^2 T^2. \end{aligned} \quad (\text{A7})$$

For the U_1 and Z' vectors, one should simply sum the $SU(4)$ Debye mass and the field dependent masses in Eq. (A6) with $n_b^L = 6, 1$. For the coloron and gluon longitudinal modes we diagonalize the following matrix:

$$m^2(\phi) + \Pi(T) = \begin{pmatrix} g_4^2\frac{\phi^2}{6} + \Pi_{H_\mu}^L(T) & -g_3g_4\frac{\phi^2}{6} \\ -g_3g_4\frac{\phi^2}{6} & g_3^2\frac{\phi^2}{6} + \Pi_{C_\mu}^L(T) \end{pmatrix}, \quad (\text{A8})$$

with $n_b^L = 8$.

⁷ We also neglect scalar Debye masses as any field dependent contribution to the potential is always suppressed by the small quartic coupling.

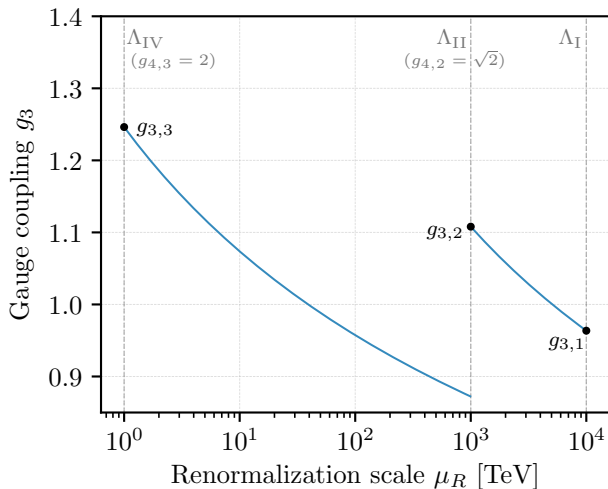


FIG. 4. The running of the $SU(3)$ gauge coupling g_3 in different phases of PS^3 . The input values $g_{4,2}(\Lambda_{II}) = \sqrt{2}$ and $g_{4,3}(\Lambda_{IV}) = 2$ correspond to the B -anomalies inspired benchmark point of Fig. 2.

Appendix B: Gauge coupling running

Here we show that the renormalization group evolution of PS^3 unambiguously determines the values of all gauge couplings at the scales of interest once the values of the $SU(4)$ gauge coupling at the second and third sites $g_{4,2}(\Lambda_{II})$ and $g_{4,3}(\Lambda_{IV})$ are specified. This is because one must match onto the strong gauge coupling at the scale Λ_{IV}

$$\frac{1}{g_s^2(\Lambda_{IV})} = \frac{1}{g_{4,3}^2(\Lambda_{IV})} + \frac{1}{g_{3,3}^2(\Lambda_{IV})}, \quad (\text{B1})$$

which determines $g_{3,3}(\Lambda_{IV})$ once $g_{4,3}(\Lambda_{IV})$ is specified. This gives the initial condition for the running of the $SU(3)_{12}$ coupling, which is relevant in the phase of theory up to Λ_{II} . At the scale of the second site Λ_{II} , the coupling $g_{3,2}(\Lambda_{II})$ is determined by an analogous matching condition after the specification of $g_{4,2}(\Lambda_{II})$. The running of $SU(3)_1$ is then determined up to the scale of the first site Λ_I , where the matching condition is simply $g_{3,1}(\Lambda_I) = g_{4,1}(\Lambda_I)$. Thus, we have the values of all gauge couplings relevant for the GW calculation, namely the values of the $SU(4)$ and $SU(3)$ gauge couplings at the scales Λ_I , Λ_{II} , and Λ_{IV} where $SU(4)$'s are broken.

We show in Fig. 4 an example running of the $SU(3)$ gauge coupling g_3 in the relevant phases of the theory, where we have taken $g_{4,3}(\Lambda_{IV}) = 2$ as suggested for compatibility with flavor anomalies. The running of g_3 was determined using the one-loop beta function

$$(4\pi)^2 \beta_{g_3} = -\mathcal{C} g_3^3, \quad (\text{B2})$$

where \mathcal{C} is a coefficient depending on the matter content. In the phase of the theory between Λ_{IV} and Λ_{II} , the rel-

evant matter content is that of Ref. [71]. Specifically, we include two pairs of Dirac fermions in the fundamental representation of $SU(3)_{12}$ in addition to a complex scalar in $(\mathbf{4}, \mathbf{3})$, resulting in $\mathcal{C} = 23/3$. When running from Λ_{II} to Λ_I the matter content is the same except with only one pair of Dirac fermions charged under $SU(3)_1$, yielding $\mathcal{C} = 27/3$.

Appendix C: Gravitational wave spectrum

Before turning to the calculation of the GW spectrum we must first specify the last remaining ingredient to calculate α , namely the effective number of relativistic degrees of freedom, g_* , in the plasma. In PS^3 this is dominated by the new gauge degrees of freedom plus the usual SM fields. We find $g_*^I \simeq 250$, $g_*^{II} \simeq 220$ and $g_*^{IV} \simeq 150$ for the three transitions.

To determine the GW spectra from the particle physics outputs, namely α , β/H and T_n as well as the choice of bubble wall velocity v_w , we utilize the recommendations from the LISA cosmology working group [2]. Here, fitting functions are given for the GW spectrum based on simulations of the plasma and bubble walls during the phase transition [91–93]. Based on these recommendations we furthermore adopt the conventions of Ref. [25], implementing the GW spectrum calculation using Tab. (1) and Eqs. (19) to (26) thereof. The case relevant in the scenario considered here is GW production in a thermal plasma, that is the sound wave and turbulence contributions dominate over the scalar field contribution.

We include a suppression of the sound wave contribution given in Ref. [25], as advocated in Refs. [18, 97]. This is relevant for transitions that occur faster than a Hubble time, reducing the time acoustic sound waves have to source GWs. We use the following suppression factor $H\tau_{sw}$ in the expression for Ω_{GW}

$$H\tau_{sw} = \min \left\{ 1, \frac{4\pi^{1/3}}{\sqrt{3}} v_w \frac{H}{\beta} \left(\frac{\alpha \kappa_{sw}(\alpha)}{1 + \alpha} \right)^{-\frac{1}{2}} \right\}, \quad (\text{C1})$$

where the efficiency factor of the sound waves, $\kappa_{sw}(\alpha)$, is given in Eq. (26) of Ref. [25]. The grey envelope of the GW spectrum shown in Fig. 2 is produced with and without this suppression factor, corresponding to the lower and upper boundaries, respectively. As the sound waves are the dominant GW production mechanism, we expect this will correspond to the dominant source of uncertainty on GW production.

The final ingredients are the experimental noise and power-law integrated curves used in the signal-to-noise ratio (SNR) analysis. Again we follow Ref. [25] closely, adding CE noise curves [7], for both pessimistic and optimistic projections, as well as the proposed atom interferometer experiments [8, 9], where we have taken the power-law integrated sensitivity curves from Ref. [98]. To determine the experimentally accessible parameter space in Fig. 3 we use an SNR threshold $\rho_{th} = 5$ for both ET and CE.

- [1] **LIGO Scientific, Virgo** Collaboration, B. P. Abbott et al., *Observation of Gravitational Waves from a Binary Black Hole Merger*, *Phys. Rev. Lett.* **116** (2016), no. 6 061102, [[arXiv:1602.03837](#)].
- [2] C. Caprini et al., *Science with the space-based interferometer eLISA. II: Gravitational waves from cosmological phase transitions*, *JCAP* **1604** (2016), no. 04 001, [[arXiv:1512.06239](#)].
- [3] K. Yagi and N. Seto, *Detector configuration of DECIGO/BBO and identification of cosmological neutron-star binaries*, *Phys. Rev.* **D83** (2011) 044011, [[arXiv:1101.3940](#)]. [Erratum: *Phys. Rev.* **D95**, no. 10, 109901 (2017)].
- [4] S. Kawamura et al., *The Japanese space gravitational wave antenna: DECIGO*, *Class. Quant. Grav.* **28** (2011) 094011.
- [5] M. Punturo et al., *The Einstein Telescope: A third-generation gravitational wave observatory*, *Class. Quant. Grav.* **27** (2010) 194002.
- [6] B. Sathyaprakash et al., *Scientific Objectives of Einstein Telescope*, *Class. Quant. Grav.* **29** (2012) 124013, [[arXiv:1206.0331](#)]. [Erratum: *Class. Quant. Grav.* **30**, 079501 (2013)].
- [7] **LIGO Scientific** Collaboration, B. P. Abbott et al., *Exploring the Sensitivity of Next Generation Gravitational Wave Detectors*, *Class. Quant. Grav.* **34** (2017), no. 4 044001, [[arXiv:1607.08697](#)].
- [8] P. W. Graham, J. M. Hogan, M. A. Kasevich, and S. Rajendran, *Resonant mode for gravitational wave detectors based on atom interferometry*, *Phys. Rev.* **D94** (2016), no. 10 104022, [[arXiv:1606.01860](#)].
- [9] **MAGIS** Collaboration, P. W. Graham, J. M. Hogan, M. A. Kasevich, S. Rajendran, and R. W. Romani, *Mid-band gravitational wave detection with precision atomic sensors*, [arXiv:1711.02225](#).
- [10] B. Allen, *The Stochastic Gravity Wave Background in Inflationary Universe Models*, *Phys. Rev.* **D37** (1988) 2078.
- [11] M. S. Turner and F. Wilczek, *Relic gravitational waves and extended inflation*, *Phys. Rev. Lett.* **65** (1990) 3080–3083.
- [12] M. Maggiore, *Gravitational wave experiments and early universe cosmology*, *Phys. Rept.* **331** (2000) 283–367, [[gr-qc/9909001](#)].
- [13] D. J. Weir, *Gravitational waves from a first order electroweak phase transition: a brief review*, *Phil. Trans. Roy. Soc. Lond.* **A376** (2018), no. 2114 20170126, [[arXiv:1705.01783](#)].
- [14] D. Curtin, P. Meade, and H. Ramani, *Thermal Resummation and Phase Transitions*, *Eur. Phys. J.* **C78** (2018), no. 9 787, [[arXiv:1612.00466](#)].
- [15] A. Katz and M. Perelstein, *Higgs Couplings and Electroweak Phase Transition*, *JHEP* **07** (2014) 108, [[arXiv:1401.1827](#)].
- [16] M. J. Baker and J. Kopp, *Dark Matter Decay between Phase Transitions at the Weak Scale*, *Phys. Rev. Lett.* **119** (2017), no. 6 061801, [[arXiv:1608.07578](#)].
- [17] I. Baldes and G. Servant, *High scale electroweak phase transition: baryogenesis & symmetry non-restoration*, *JHEP* **10** (2018) 053, [[arXiv:1807.08770](#)].
- [18] J. Ellis, M. Lewicki, and J. M. No, *On the Maximal Strength of a First-Order Electroweak Phase Transition and its Gravitational Wave Signal*, [arXiv:1809.08242](#). [*JCAP* **1904**, 003 (2019)].
- [19] E. Madge and P. Schwaller, *Leptophilic dark matter from gauged lepton number: Phenomenology and gravitational wave signatures*, *JHEP* **02** (2019) 048, [[arXiv:1809.09110](#)].
- [20] A. Beniwal, M. Lewicki, M. White, and A. G. Williams, *Gravitational waves and electroweak baryogenesis in a global study of the extended scalar singlet model*, *JHEP* **02** (2019) 183, [[arXiv:1810.02380](#)].
- [21] D. Croon, T. E. Gonzalo, and G. White, *Gravitational Waves from a Pati-Salam Phase Transition*, *JHEP* **02** (2019) 083, [[arXiv:1812.02747](#)].
- [22] D. Croon, V. Sanz, and G. White, *Model Discrimination in Gravitational Wave spectra from Dark Phase Transitions*, *JHEP* **08** (2018) 203, [[arXiv:1806.02332](#)].
- [23] V. Brdar, A. J. Helmboldt, and J. Kubo, *Gravitational Waves from First-Order Phase Transitions: LIGO as a Window to Unexplored Seesaw Scales*, *JCAP* **1902** (2019) 021, [[arXiv:1810.12306](#)].
- [24] A. Addazi, A. Marcianò, and R. Pasechnik, *Probing Trans-electroweak First Order Phase Transitions from Gravitational Waves*, *MDPI Physics* **1** (2019), no. 1 92–102, [[arXiv:1811.09074](#)].
- [25] M. Breitbach, J. Kopp, E. Madge, T. Opferkuch, and P. Schwaller, *Dark, Cold, and Noisy: Constraining Secluded Hidden Sectors with Gravitational Waves*, *JCAP* **1907** (2019), no. 07 007, [[arXiv:1811.11175](#)].
- [26] A. Angelescu and P. Huang, *Multistep Strongly First Order Phase Transitions from New Fermions at the TeV Scale*, *Phys. Rev.* **D99** (2019), no. 5 055023, [[arXiv:1812.08293](#)].
- [27] A. Alves, T. Ghosh, H.-K. Guo, K. Sinha, and D. Vagie, *Collider and Gravitational Wave Complementarity in Exploring the Singlet Extension of the Standard Model*, *JHEP* **04** (2019) 052, [[arXiv:1812.09333](#)].
- [28] K. Kannike and M. Raidal, *Phase Transitions and Gravitational Wave Tests of Pseudo-Goldstone Dark Matter in the Softly Broken U(1) Scalar Singlet Model*, *Phys. Rev.* **D99** (2019), no. 11 115010, [[arXiv:1901.03333](#)].
- [29] M. Fairbairn, E. Hardy, and A. Wickens, *Hearing without seeing: gravitational waves from hot and cold hidden sectors*, *JHEP* **07** (2019) 044, [[arXiv:1901.11038](#)].
- [30] T. Hasegawa, N. Okada, and O. Seto, *Gravitational waves from the minimal gauged U(1)_{B-L} model*, *Phys. Rev.* **D99** (2019), no. 9 095039, [[arXiv:1904.03020](#)].
- [31] D. Dunskey, L. J. Hall, and K. Harigaya, *Dark Matter, Dark Radiation and Gravitational Waves from Mirror Higgs Parity*, [arXiv:1908.02756](#).
- [32] P. Athron, C. Balazs, A. Fowlie, G. Pozzo, G. White, and Y. Zhang, *Strong first-order phase transitions in the NMSSM - a comprehensive survey*, [arXiv:1908.11847](#).
- [33] S. De Curtis, L. Delle Rose, and G. Panico, *Composite Dynamics in the Early Universe*, [arXiv:1909.07894](#).
- [34] A. Addazi, A. Marcianò, A. P. Morais, R. Pasechnik, R. Srivastava, and J. W. F. Valle, *Gravitational footprints of massive neutrinos and lepton number breaking*, [arXiv:1909.09740](#).

- [35] T. Alanne, T. Hogle, M. Platscher, and K. Schmitz, *A fresh look at the gravitational-wave signal from cosmological phase transitions*, [arXiv:1909.11356](#).
- [36] T. Vachaspati and A. Vilenkin, *Gravitational Radiation from Cosmic Strings*, *Phys. Rev.* **D31** (1985) 3052.
- [37] T. Damour and A. Vilenkin, *Gravitational radiation from cosmic (super)strings: Bursts, stochastic background, and observational windows*, *Phys. Rev.* **D71** (2005) 063510, [[hep-th/0410222](#)].
- [38] J. J. Blanco-Pillado, K. D. Olum, and B. Shlaer, *The number of cosmic string loops*, *Phys. Rev.* **D89** (2014), no. 2 023512, [[arXiv:1309.6637](#)].
- [39] J. A. Dror, T. Hiramatsu, K. Kohri, H. Murayama, and G. White, *Testing Seesaw and Leptogenesis with Gravitational Waves*, [arXiv:1908.03227](#).
- [40] S. Y. Khlebnikov and I. I. Tkachev, *Relic gravitational waves produced after preheating*, *Phys. Rev.* **D56** (1997) 653–660, [[hep-ph/9701423](#)].
- [41] R. Easther and E. A. Lim, *Stochastic gravitational wave production after inflation*, *JCAP* **0604** (2006) 010, [[astro-ph/0601617](#)].
- [42] R. Easther, J. T. Giblin, Jr., and E. A. Lim, *Gravitational Wave Production At The End Of Inflation*, *Phys. Rev. Lett.* **99** (2007) 221301, [[astro-ph/0612294](#)].
- [43] J. Garcia-Bellido and D. G. Figueroa, *A stochastic background of gravitational waves from hybrid preheating*, *Phys. Rev. Lett.* **98** (2007) 061302, [[astro-ph/0701014](#)].
- [44] J. Garcia-Bellido, D. G. Figueroa, and A. Sastre, *A Gravitational Wave Background from Reheating after Hybrid Inflation*, *Phys. Rev.* **D77** (2008) 043517, [[arXiv:0707.0839](#)].
- [45] J.-F. Dufaux, G. Felder, L. Kofman, and O. Navros, *Gravity Waves from Tachyonic Preheating after Hybrid Inflation*, *JCAP* **0903** (2009) 001, [[arXiv:0812.2917](#)].
- [46] C. S. Machado, W. Ratzinger, P. Schwaller, and B. A. Stefanek, *Audible Axions*, *JHEP* **01** (2019) 053, [[arXiv:1811.01950](#)].
- [47] M. Sasaki, T. Suyama, T. Tanaka, and S. Yokoyama, *Primordial black holes—perspectives in gravitational wave astronomy*, *Class. Quant. Grav.* **35** (2018), no. 6 063001, [[arXiv:1801.05235](#)].
- [48] L. Barack et al., *Black holes, gravitational waves and fundamental physics: a roadmap*, *Class. Quant. Grav.* **36** (2019), no. 14 143001, [[arXiv:1806.05195](#)].
- [49] N. Bartolo, V. De Luca, G. Franciolini, M. Peloso, D. Racco, and A. Riotto, *Testing primordial black holes as dark matter with LISA*, *Phys. Rev.* **D99** (2019), no. 10 103521, [[arXiv:1810.12224](#)].
- [50] B. Grinstein, M. Redi, and G. Villadoro, *Low Scale Flavor Gauge Symmetries*, *JHEP* **11** (2010) 067, [[arXiv:1009.2049](#)].
- [51] R. Alonso, M. B. Gavela, G. Isidori, and L. Maiani, *Neutrino Mixing and Masses from a Minimum Principle*, *JHEP* **11** (2013) 187, [[arXiv:1306.5927](#)].
- [52] D. Guadagnoli, R. N. Mohapatra, and I. Sung, *Gauged Flavor Group with Left-Right Symmetry*, *JHEP* **04** (2011) 093, [[arXiv:1103.4170](#)].
- [53] R. Alonso, M. B. Gavela, L. Merlo, and S. Rigolin, *On the scalar potential of minimal flavour violation*, *JHEP* **07** (2011) 012, [[arXiv:1103.2915](#)].
- [54] R. Alonso, M. B. Gavela, D. Hernandez, and L. Merlo, *On the Potential of Leptonic Minimal Flavour Violation*, *Phys. Lett.* **B715** (2012) 194–198, [[arXiv:1206.3167](#)].
- [55] E. Nardi, *Naturally large Yukawa hierarchies*, *Phys. Rev.* **D84** (2011) 036008, [[arXiv:1105.1770](#)].
- [56] J. R. Espinosa, C. S. Fong, and E. Nardi, *Yukawa hierarchies from spontaneous breaking of the $SU(3)_L \times SU(3)_R$ flavour symmetry?*, *JHEP* **02** (2013) 137, [[arXiv:1211.6428](#)].
- [57] T. Feldmann, F. Hartmann, W. Kilian, and C. Luhn, *Combining Pati-Salam and Flavour Symmetries*, *JHEP* **10** (2015) 160, [[arXiv:1506.00782](#)].
- [58] F. Bishara, A. Greljo, J. F. Kamenik, E. Stamou, and J. Zupan, *Dark Matter and Gauged Flavor Symmetries*, *JHEP* **12** (2015) 130, [[arXiv:1505.03862](#)].
- [59] A. Crivellin, J. Fuentes-Martin, A. Greljo, and G. Isidori, *Lepton Flavor Non-Universality in B decays from Dynamical Yukawas*, *Phys. Lett.* **B766** (2017) 77–85, [[arXiv:1611.02703](#)].
- [60] M. Bordone, C. Cornella, J. Fuentes-Martin, and G. Isidori, *A three-site gauge model for flavor hierarchies and flavor anomalies*, *Phys. Lett.* **B779** (2018) 317–323, [[arXiv:1712.01368](#)].
- [61] **BaBar** Collaboration, J. P. Lees et al., *Measurement of an Excess of $\bar{B} \rightarrow D^{(*)} \tau^- \bar{\nu}_\tau$ Decays and Implications for Charged Higgs Bosons*, *Phys. Rev.* **D88** (2013), no. 7 072012, [[arXiv:1303.0571](#)].
- [62] **Belle** Collaboration, S. Hirose et al., *Measurement of the τ lepton polarization and $R(D^*)$ in the decay $\bar{B} \rightarrow D^* \tau^- \bar{\nu}_\tau$* , *Phys. Rev. Lett.* **118** (2017), no. 21 211801, [[arXiv:1612.00529](#)].
- [63] **LHCb** Collaboration, R. Aaij et al., *Measurement of the ratio of branching fractions $\mathcal{B}(\bar{B}^0 \rightarrow D^{*+} \tau^- \bar{\nu}_\tau) / \mathcal{B}(\bar{B}^0 \rightarrow D^{*+} \mu^- \bar{\nu}_\mu)$* , *Phys. Rev. Lett.* **115** (2015), no. 11 111803, [[arXiv:1506.08614](#)]. [Erratum: *Phys. Rev. Lett.* 115, no. 15, 159901 (2015)].
- [64] **LHCb** Collaboration, R. Aaij et al., *Test of lepton universality using $B^+ \rightarrow K^+ \ell^+ \ell^-$ decays*, *Phys. Rev. Lett.* **113** (2014) 151601, [[arXiv:1406.6482](#)].
- [65] **LHCb** Collaboration, R. Aaij et al., *Test of lepton universality with $B^0 \rightarrow K^{*0} \ell^+ \ell^-$ decays*, *JHEP* **08** (2017) 055, [[arXiv:1705.05802](#)].
- [66] **LHCb** Collaboration, R. Aaij et al., *Measurement of Form-Factor-Independent Observables in the Decay $B^0 \rightarrow K^{*0} \mu^+ \mu^-$* , *Phys. Rev. Lett.* **111** (2013) 191801, [[arXiv:1308.1707](#)].
- [67] **LHCb** Collaboration, R. Aaij et al., *Angular analysis of the $B^0 \rightarrow K^{*0} \mu^+ \mu^-$ decay using 3 fb^{-1} of integrated luminosity*, *JHEP* **02** (2016) 104, [[arXiv:1512.04442](#)].
- [68] **LHCb** Collaboration, R. Aaij et al., *Search for lepton-universality violation in $B^+ \rightarrow K^+ \ell^+ \ell^-$ decays*, *Phys. Rev. Lett.* **122** (2019), no. 19 191801, [[arXiv:1903.09252](#)].
- [69] D. Buttazzo, A. Greljo, G. Isidori, and D. Marzocca, *B-physics anomalies: a guide to combined explanations*, *JHEP* **11** (2017) 044, [[arXiv:1706.07808](#)].
- [70] L. Di Luzio, A. Greljo, and M. Nardecchia, *Gauge leptoquark as the origin of B-physics anomalies*, *Phys. Rev.* **D96** (2017), no. 11 115011, [[arXiv:1708.08450](#)].
- [71] A. Greljo and B. A. Stefanek, *Third family quark–lepton unification at the TeV scale*, *Phys. Lett.* **B782** (2018) 131–138, [[arXiv:1802.04274](#)].
- [72] M. Bordone, C. Cornella, J. Fuentes-Martin, and G. Isidori, *Low-energy signatures of the PS^3 model:*

- from *B*-physics anomalies to LFV, *JHEP* **10** (2018) 148, [[arXiv:1805.09328](#)].
- [73] C. Cornella, J. Fuentes-Martin, and G. Isidori, *Revisiting the vector leptoquark explanation of the B-physics anomalies*, *JHEP* **07** (2019) 168, [[arXiv:1903.11517](#)].
- [74] J. Fuentes-Martín, M. Reig, and A. Vicente, *4321... axion!*, [arXiv:1907.02550](#).
- [75] J. C. Pati and A. Salam, *Lepton Number as the Fourth Color*, *Phys. Rev.* **D10** (1974) 275–289. [Erratum: *Phys. Rev.* **D11**, 703(1975)].
- [76] N. Arkani-Hamed, A. G. Cohen, and H. Georgi, *Electroweak symmetry breaking from dimensional deconstruction*, *Phys. Lett.* **B513** (2001) 232–240, [[hep-ph/0105239](#)].
- [77] R. Jeannerot, S. Khalil, G. Lazarides, and Q. Shafi, *Inflation and monopoles in supersymmetric $SU(4)C \times SU(2)(L) \times SU(2)(R)$* , *JHEP* **10** (2000) 012, [[hep-ph/0002151](#)].
- [78] R. Barbieri, G. Isidori, J. Jones-Perez, P. Lodone, and D. M. Straub, *$U(2)$ and Minimal Flavour Violation in Supersymmetry*, *Eur. Phys. J.* **C71** (2011) 1725, [[arXiv:1105.2296](#)].
- [79] G. Valencia and S. Willenbrock, *Quark - lepton unification and rare meson decays*, *Phys. Rev.* **D50** (1994) 6843–6848, [[hep-ph/9409201](#)].
- [80] A. D. Smirnov, *Mass limits for scalar and gauge leptoquarks from $K(L)0 \rightarrow e^- + \mu^\pm$, $B0 \rightarrow e^- + \tau^\pm$ decays*, *Mod. Phys. Lett.* **A22** (2007) 2353–2363, [[arXiv:0705.0308](#)].
- [81] A. V. Kuznetsov, N. V. Mikheev, and A. V. Serghienko, *The third type of fermion mixing in the lepton and quark interactions with leptoquarks*, *Int. J. Mod. Phys.* **A27** (2012) 1250062, [[arXiv:1203.0196](#)].
- [82] G. F. Giudice, G. Isidori, A. Salvio, and A. Strumia, *Softened Gravity and the Extension of the Standard Model up to Infinite Energy*, *JHEP* **02** (2015) 137, [[arXiv:1412.2769](#)].
- [83] A. D. Smirnov, *Vector leptoquark mass limits and branching ratios of $K_L^0, B^0, B_s \rightarrow l_i^+ l_j^-$ decays with account of fermion mixing in leptoquark currents*, [arXiv:1801.02895](#).
- [84] W. D. Goldberger and M. B. Wise, *Modulus stabilization with bulk fields*, *Phys. Rev. Lett.* **83** (1999) 4922–4925, [[hep-ph/9907447](#)].
- [85] N. Arkani-Hamed, H.-C. Cheng, P. Creminelli, and L. Randall, *Extra natural inflation*, *Phys. Rev. Lett.* **90** (2003) 221302, [[hep-th/0301218](#)].
- [86] M. S. Turner, E. J. Weinberg, and L. M. Widrow, *Bubble nucleation in first order inflation and other cosmological phase transitions*, *Phys. Rev.* **D46** (1992) 2384–2403.
- [87] M. Kamionkowski, A. Kosowsky, and M. S. Turner, *Gravitational radiation from first order phase transitions*, *Phys. Rev.* **D49** (1994) 2837–2851, [[astro-ph/9310044](#)].
- [88] C. Grojean and G. Servant, *Gravitational Waves from Phase Transitions at the Electroweak Scale and Beyond*, *Phys. Rev.* **D75** (2007) 043507, [[hep-ph/0607107](#)].
- [89] C. L. Wainwright, *CosmoTransitions: Computing Cosmological Phase Transition Temperatures and Bubble Profiles with Multiple Fields*, *Comput. Phys. Commun.* **183** (2012) 2006–2013, [[arXiv:1109.4189](#)].
- [90] J. R. Espinosa, *A Fresh Look at the Calculation of Tunneling Actions*, *JCAP* **1807** (2018), no. 07 036, [[arXiv:1805.03680](#)].
- [91] S. J. Huber and T. Konstandin, *Gravitational Wave Production by Collisions: More Bubbles*, *JCAP* **0809** (2008) 022, [[arXiv:0806.1828](#)].
- [92] M. Hindmarsh, S. J. Huber, K. Rummukainen, and D. J. Weir, *Numerical simulations of acoustically generated gravitational waves at a first order phase transition*, *Phys. Rev.* **D92** (2015), no. 12 123009, [[arXiv:1504.03291](#)].
- [93] C. Caprini, R. Durrer, and G. Servant, *The stochastic gravitational wave background from turbulence and magnetic fields generated by a first-order phase transition*, *JCAP* **0912** (2009) 024, [[arXiv:0909.0622](#)].
- [94] E. Thrane and J. D. Romano, *Sensitivity curves for searches for gravitational-wave backgrounds*, *Phys. Rev.* **D88** (2013), no. 12 124032, [[arXiv:1310.5300](#)].
- [95] D. Comelli and J. R. Espinosa, *Bosonic thermal masses in supersymmetry*, *Phys. Rev.* **D55** (1997) 6253–6263, [[hep-ph/9606438](#)].
- [96] M. Laine and A. Vuorinen, *Basics of Thermal Field Theory*, *Lect. Notes Phys.* **925** (2016) pp.1–281, [[arXiv:1701.01554](#)].
- [97] M. Hindmarsh, S. J. Huber, K. Rummukainen, and D. J. Weir, *Shape of the acoustic gravitational wave power spectrum from a first order phase transition*, *Phys. Rev.* **D96** (2017), no. 10 103520, [[arXiv:1704.05871](#)].
- [98] J. Ellis, M. Lewicki, J. M. No, and V. Vaskonen, *Gravitational wave energy budget in strongly supercooled phase transitions*, *JCAP* **1906** (2019), no. 06 024, [[arXiv:1903.09642](#)].